



Deposited via The University of Sheffield.

White Rose Research Online URL for this paper:

<https://eprints.whiterose.ac.uk/id/eprint/146694/>

Version: Accepted Version

Article:

Bondar, D., Ma, Q., Soutsos, M. et al. (2018) Alkali activated slag concretes designed for a desired slump, strength and chloride diffusivity. *Construction and Building Materials*, 190. pp. 191-199. ISSN: 0950-0618

<https://doi.org/10.1016/j.conbuildmat.2018.09.124>

Article available under the terms of the CC-BY-NC-ND licence
(<https://creativecommons.org/licenses/by-nc-nd/4.0/>).

Reuse

This article is distributed under the terms of the Creative Commons Attribution-NonCommercial-NoDerivs (CC BY-NC-ND) licence. This licence only allows you to download this work and share it with others as long as you credit the authors, but you can't change the article in any way or use it commercially. More information and the full terms of the licence here: <https://creativecommons.org/licenses/>

Takedown

If you consider content in White Rose Research Online to be in breach of UK law, please notify us by emailing eprints@whiterose.ac.uk including the URL of the record and the reason for the withdrawal request.

Alkali activated slag concretes designed for a desired slump, strength and chloride diffusivity

Dali Bondar¹, Qianmin Ma², Marios Soutsos¹, Muhammed Basheer³, John L. Provis⁴, Sreejith Nanukuttan¹

¹School of Natural and Built Environment, Queen's University Belfast, BT9 5AG, UK

²Faculty of Civil Engineering and Mechanics, Kunming University of Science and Technology, 650500 Kunming, China

³School of Civil Engineering, University of Leeds, LS2 9JT, UK

⁴Department of Materials Science and Engineering, University of Sheffield, S1 3JD, UK

Email: d.bondar@qub.ac.uk, maqianmin666@163.com, m.soutsos@qub.ac.uk,
P.A.M.Basheer@leeds.ac.uk, J.Provis@Sheffield.ac.uk, s.nanukuttan@qub.ac.uk

Abstract

Ground granulated blast furnace slag (GGBS) is the most common industrial by-product used as a precursor for alkali activated binders due to its fast setting, simple curing needs, and good early age strength gain. There are conflicting findings on the chloride penetration resistance of such binders and more information is required regarding the suitability of this type of binder material for chloride environments. This article outlines the findings of investigation of alkali activated slag concretes (AASC), to provide a comprehensive view of the effect of mix design variables on slump, strength, and chloride transport and binding. It is concluded that AASC can be designed for different workability and different grades of concrete. The diffusivity results demonstrate that the addition of excess water does not directly control the pore structure/connectivity in AASC as it does for Portland cement, and therefore AASC can be designed based on the water/binder ratio needed for a specified mechanical performance. The chloride binding capacity increased as the paste content of the concrete and/or the silica content of the activator was increased.

Keywords: alkali activated slag concretes (AASC); workability; strength; chloride diffusion and chloride binding capacity

1. Introduction

Alkali activated materials (AAMs) have been under consideration as an alternative binder system since 1895 [1]. However, despite the engineering community having been aware of the potential of this material for over a century, there is still insufficient information available about the durability of AAMs, and the resistance to chloride ingress is particularly critical for materials intended to serve in reinforced concretes.

Several factors are known to affect the setting time, workability, strength and durability properties of alkali activated slag concretes (AASC), including: the type of alkaline activator, the means of adding the activator, the dosage of alkali, the SiO₂/Na₂O ratio (denoted *modulus*, Ms), the type and fineness of slag, the paste content of the concrete, and the water to solid ratio in the paste constituent of AASC.

36 Many of these factors are interdependent, and the effect of changing more than one in parallel is usually
37 not additive. The optimum Na_2O dosage for AAS binders activated by sodium silicate solution under
38 normal curing has been found to be 3% – 5% relative to the mass of slag, depending on the demand for
39 high early age strength [2-4]. Slag cements activated by sodium silicate at modulus values between 0.6
40 and 1.5 at appropriate dosages were reported to show high ultimate strength for engineering purposes.
41 However, this optimum modulus for appropriate dosage of sodium silicate varied depending on the type
42 of slag, i.e. 0.75 – 1.25 for acid slag, 0.90 – 1.3 for neutral slag, and 1.0 – 1.5 for basic slag [3-5].
43 Activation by sodium silicate tends to give higher strength than when NaOH is used; the lower strength
44 in the NaOH activated slag pastes may be explained by the much higher porosity found in these pastes
45 than in the sodium silicate activated materials [6].

46 The effect of water to slag ratio on NaOH activated slag is similar to that of water to cement ratio on
47 Portland cement [4]. However, an increase in water to slag ratio has a very marked effect to decrease
48 the heat evolution of Na_2SiO_3 activated slag [4]. In this case when the water to solid/slag ratio is lower
49 than 0.45, there is an early and pronounced peak in the heat evolution curve, which then changes to a
50 very diffuse peak with 15 hours delay for a water to slag ratio greater than 0.45 [4]. This can have a
51 noticeable effect on the performance of AASC, especially on workability and setting time.

52 It has been reported [7] that by controlling mix design parameters, such as binder content and water to
53 binder ratio, it is possible to produce AASC with mechanical strength and durability comparable to
54 conventional Portland cement concretes. It has also been shown that a higher slag content leads to an
55 increase in strength of AASC and improvement of the permeability, water absorption and carbonation
56 resistance [7].

57 Park *et al.* [8], in their work using mortars, have reported that the corrosion behaviour of embedded
58 steel in AAMs was strongly dependent on the type of alkali activator. According to their findings, AAS
59 containing $\text{Ca}(\text{OH})_2$ as the activator was most effective to reduce galvanic corrosion, while KOH and
60 NaOH activators indicated corrosion levels similar to that of Portland cement mortar [8].

61 AASC has traditionally been known for its low slump, and this raises challenges in its design for
62 different workabilities and different grades of concrete. Therefore, this article presents findings from
63 investigations of the effect of water/slag ratio and binder content on workability, strength, chloride
64 diffusion and chloride binding in AASC, with the aim of determining the suitability of AASC for use
65 in chloride environments. The outcomes will help designers to select mix designs for AASC for required
66 performance.

67

68

69

70 **2. Materials and experimental procedures**

71 **2.1 Materials**

72 The granulated blast furnace slag used in this study was provided by ECOCEM, France. The basicity
73 coefficient $(\text{CaO}+\text{MgO}/\text{SiO}_2+\text{Al}_2\text{O}_3)$ and the quality coefficient $(\text{CaO}+\text{MgO}+\text{Al}_2\text{O}_3)/(\text{SiO}_2+\text{TiO}_2)$ were
74 calculated from the chemical composition (Table 1) to be 1.07 and 1.7, respectively. The particle size
75 distribution of slag was determined by laser diffraction, the particle density was measured using a
76 LeChatelier flask, and the water absorption was measured using the centrifugal consolidation method;
77 these physical properties are presented in Table 2.

78 The aggregates used in this study were crushed basalt from local sources in Northern Ireland, and
79 comprised 10 mm and 16.5 mm crushed aggregates, and 4 mm sand. In stage A of the experimental
80 campaign, the proportion of 16.5:10:4 mm fractions were 32:32:36; in stage B the proportions were
81 optimised for the best packing density at 48:12:40. The bulk specific gravity and water absorption of
82 these materials were measured based on BS EN 1097-1, and are presented in Table 3. Potable tap water
83 (i.e. drinking water quality) was used to make the concrete mixes.

84 Sodium hydroxide (NaOH) pellets were dissolved in water and used along with sodium silicate solution
85 to act as alkaline activators in concrete production at specified concentrations and compositions, as
86 shown in Table 4. The chemical composition of the as-received sodium silicate solution was 15.5%
87 sodium oxide (Na_2O), 30.5% silicon dioxide (SiO_2) and 54% water, on a mass basis. NaOH was used
88 to adjust the Na_2O content and Ms value to the required values.

89 **2.2 Mix details, mixing and casting of test specimens**

90 Twelve AAS concretes with alkali concentrations (Na_2O % by of mass of slag) of 4, 6, and 8 %, and
91 modulus (Ms) values of the sodium silicate solution activator of 0.75, 1.00, 1.50, and 2.00, were studied
92 in stage A. The water/binder mass ratio (w/b) was held constant at 0.47 in these concretes. A barium
93 based retarder was used in this work for mixes A1-A12 for controlling the setting time. The content of
94 the retarder was 0.3% of the mass of slag for all of these mixes and dry-blended with slag before mixing.
95 For the purpose of comparison, one PC concrete mix was manufactured with the same total binder
96 content as that of the AAS concretes. A w/b of 0.42 was specified for the PC concrete [9] to ensure that
97 its performance in exposure classes XS3 and XD3 as defined in BS EN 206:2013 [10] would be
98 acceptable. In stage B, ten further AAS concretes were studied with different w/b ratios, binder to
99 aggregate ratios, alkali concentrations, and Ms values without using retarder. The details of the different
100 mixes and their initial properties are presented in Table 4. Throughout this work, the total binder content
101 is defined as the sum of GGBS and the solid component of the sodium silicate solution, and the water
102 content of the sodium silicate solution was taken into account while determining the mixing water.

103 A laboratory pan-mixer of volume 50 L was used in this study. In stage A the mixing was conducted in
104 accordance with BS 1881-125:2013 [11]. In Stage B, crushed basalt aggregates and sand were first dry-
105 mixed together for one minute, and the GGBS powder was subsequently added, and mixed for a further
106 2 minutes. The sodium hydroxide solution was then added and after a further 2 minutes of mixing, then
107 sodium silicate solution was added and mixing continued for a further minute.

108 For both stages, fresh properties of concrete were measured according to BS EN 12350 [12], and nine
109 100 mm cubes and one 250×250×110 mm slab were cast for determining compressive strength in
110 accordance with BS EN 12390 [13], and chloride diffusion coefficients according to Nordtest NT Build
111 443 [14]. After casting, all the specimens (still in moulds) were covered with plastic sheets and left in
112 the casting room for 24 h. The demoulded slabs were wrapped with 3 layers of plastic sheets, and cube
113 samples were kept in a sealed plastic zip bag, until the testing date. The storage room was maintained
114 at 23°C and 65% RH.

115 **2.3 Testing procedures**

116 Chloride transport through AAS concretes was assessed using a non-steady state chloride diffusion test,
117 Nordtest NT Build 443 [14]. One day before the test age of 91 days, three cores of diameter 100 mm
118 per mix were drilled from the 250 x 250 x 110 mm concrete blocks. A slice with a thickness of 50 mm
119 from the cast surface (trowel finished face) was cut off, and the rest was kept for carrying out the test.
120 The vacuum saturation regime specified in the standard was used to precondition the slices so that the
121 chloride flow is predominantly diffusive, and initial sorption or capillary forces are negligible. The
122 vacuum was applied to remove air for three hours and released afterwards. Samples were wrapped in
123 hessian saturated in deionised water to prevent leaching of ions, and placed in the container. The weight
124 of the sample was noted after an hour (W_1) and then vacuum was applied, followed by further saturation.
125 Weight was checked again (W_2). Usually after 6 hours, when $W_i - W_{(i-1)}$ was less than 0.1%, the samples
126 were considered fully saturated; if not, saturation was continued until this criterion was met. After
127 conditioning to a surface-dry condition, an epoxy resin was applied onto the surfaces of the specimens
128 in three layers except the exposure face (saw cut face). When the epoxy coating was dry, the cores were
129 immersed in an NaCl solution of concentration 165 g/L (~2.82 M) for three months for samples tested
130 in stage A, or six months for samples tested in stage B. After immersion, the cores were profile ground
131 to obtain concrete dust from different depths up to a depth of 30 mm in stage A and 16 mm in stage B,
132 measured from the exposed surface. The total chloride content of the dust samples was determined in
133 accordance with the recommendations of RILEM TC 178-TMC [15] using a pre-calibrated
134 potentiometric titration method. The concrete dust was dissolved in deionised water in accordance with
135 RILEM TC 178-TMC recommendations [16] to measure the pH value of the suspension in both stages,
136 and for the determination of water soluble chlorides in stage B. Chloride diffusivity and the surface

137 chloride content were determined by using curve fitting to the error function solution of Fick's second
138 law of diffusion, as described in NT BUILD 443 [14].

139 **3. Results and discussion**

140 The following sections discuss the slump, compressive strength, chloride diffusivity, and chloride
141 binding capacity of AAS concretes.

142 **3.1 Slump**

143 AASC has often been characterised by a low slump value and rapid setting behaviour; slump values up
144 to 60-120 mm have been reported in the literature [17]. The purpose of this testing programme was to
145 demonstrate the range of slump values that AASC is capable of producing, and the changes to the
146 governing variables that are necessary to achieve such high slump. The Stage A results shown in Table
147 4 and Figure 1 indicate that a slump value between 55-180 mm can be achieved by varying the
148 percentage Na_2O and M_s while the w/b is fixed at 0.47. As the percentage of Na_2O increased, the slump
149 increased from 55-70 mm (Mixes A1, A5 and A9), and a further increase in modulus (A1-A4, A5-A8,
150 A9-12) brought the slump values to 180 mm due to the plasticising effects of dissolved silicate anions.
151 In order to design slump class $\geq S3$ specified in BS 8500-1:2015 [18], an Na_2O dose of 8% is required.
152 The role of parameters such as $\text{Na}_2\text{O}\%$ and M_s in controlling the slump has been widely reported in the
153 literature [19, 20] and is in agreement with the Stage A results.

154 In Stage B, tests were designed to consider the effects of other parameters such as w/b and binder
155 content and did not use the retarder. Mixes in this stage were limited to M_s values of 0.45 or 1, as an
156 increase in modulus means a proportional increase in the sodium silicate content, which is both costly
157 and can have high negative environmental impacts. The main difference between the mix designs in the
158 two stages is that w/b was increased to 0.55 in stage B, and its effect is very obvious on the slump as
159 mixes B4, B6-B10 had slump values in excess of 135 mm. What is more interesting is that slump values
160 >200 mm are achievable with low $\text{Na}_2\text{O}\%$ and M_s by increasing w/b, so in this sense, the AASC behaves
161 similarly to PC concretes without any observation of bleeding or segregation.

162 As is evident from Figure 1a and 1b, the AASC can be designed for all slump ranges. However, higher
163 slumps in the range of S4-S5 require w/b ratios higher than those allowed in BS 8500 [18]. Whether
164 such high w/b ratios are acceptable for concretes in different chloride exposure environments will be
165 further discussed in section 3.3, after the diffusivity results are presented.

166 The contour map graphs in Figure 2 show the results obtained for slump as a function of sodium oxide
167 ($\text{Na}_2\text{O}\%$) and silicate modulus (M_s), for different mixes with same binder content for both stages. Using
168 a w/b ratio of 0.55 instead of 0.47 resulted in more workable mixes. It is obvious from Figure 2(b) that
169 at higher w/b, both sodium oxide ($\text{Na}_2\text{O}\%$) & silica modulus (M_s) have a significant effect on
170 workability, while for lower w/b, parallel lines in Figure 2 (a) indicates that only the effect of $\text{Na}_2\text{O}\%$

171 is significant. All AAS concrete mixes in stage 2 (i.e., 0.55 w/b) are in at least class S3 specified in BS
172 8500-1:2015 [18], even for the minimum alkali content and silica modulus, which are 4% and 0.45,
173 respectively in this stage, whereas in stage A the minimum alkali content to reach this class of
174 workability was more than 7.5% and the minimum silica modulus is 1.0. It is evident from the results
175 in stage B that for a silica modulus more than 0.8, increasing the sodium oxide increases the workability,
176 as has been reported by previous investigators [18, 19].

177 3.2 Compressive strength

178 An overall comparison of the results between Stages A and B (Figure 3) makes the effect of w/b very
179 apparent, with almost all (except one) Stage A mixes exceeding 45 MPa at 28 days. Stage B mixes with
180 w/b between 0.55 and 0.7 offer 28-day compressive strengths in the range 21.5 to 64.4 MPa. From the
181 Stage A results, it can also be stated that: (1) most mixes had approximately 20 MPa after 3 days curing,
182 (2) higher modulus results in loss of early strength, but offers comparable strength in the long term, (3)
183 in most cases 28 day strength is 80-90% of the 91 day strength, offering insight into the short and long
184 term microstructural development in such binders. It is obvious that mixes with high modulus (i.e.,
185 silicate content) need to be cured longer. Concretes with Ms values of 1.0 to 1.5 generally obtained the
186 highest compressive strength (see Figure 3(a)), which is in agreement with the literature [21].

187 Figure 3b shows data for mixes with varying w/b. The comparable mixes B8-10 all offer better strengths
188 than their Stage A equivalents (A2, A6, A10) after 28 days, despite their higher w/b. But as time
189 progress, i.e., with 91 days curing, the aforementioned differences become negligible. Better strengths
190 for Stage B could be due to their higher density. Due to these differences, it is best to summarise that
191 strength in the range of 20-60 MPa is achievable by altering the binder content, w/b, Ms, and Na₂O%.
192 To aid with the design for strength, a contour map using 28 day compressive strength results as a
193 function of sodium oxide (Na₂O%) and silica modulus (Ms) is provided in Figure 4. An increase of
194 Na₂O% and Ms generally increases the compressive strength, which is in agreement with the results
195 reported by others [19, 21]. This is due to the higher degree of reaction (indicating the extent to which
196 the slag particles are reacted) caused by an increase in the alkali activator dosage [22]. More N-A-S-H
197 (sodium aluminosilicate hydrate) gels are generated when the Na₂O% and SiO₂ content are increased.
198 The bottom right corner of Figure 4a (Stage A results) also shows that the strength value decreases as
199 the silica modulus increases beyond 1.5 for Na₂O doses below 5%, as the alkalinity of the activators in
200 such systems is not sufficient to reach a very high degree of reaction.

201 The PC concrete in Stage A was designed as a reference that conforms to the BS EN 206:2013
202 requirement for exposure classes XS3 and XD3. Therefore, it was designed for a minimum
203 characteristic compressive strength of 45 MPa, which is equivalent to an average strength ≥ 49.41 MPa
204 (calculated as $45 + 1.48(3.15)$ MPa; where 3.15 is the standard deviation of the test results). Table 4 and
205 Figure 3(a) both show that mixes no. A3(4%-1.5), A6(6%-1.0), A7(6%-1.5), A8(6%-2), A9 (8%-0.75),

206 A10 (8%-1.0), A11(8%-1.5), A12(8%-2) and the PC met the strength requirements for this exposure
207 class. Additionally, most of the AAS concretes except mix A4(4%-2) met the strength requirement of
208 41.66 (=37+1.48(3.15)) MPa for the lower-demand exposure classes XS1, XD1 and XD2. It should be
209 noted that the w/b ratio used for AAS concretes (0.47) was higher than that for PC concrete (0.42) due
210 to the lack of workability of the AAS at such a low water content [9]. The 28 day compressive strength
211 results reported for stage B in Table 4 and Figure 3(b) show that mixes B7(8%-0.45), B9(6%-1) and
212 B10(8%-1) also achieved the required strength ≥ 51.11 (=45+1.48(4.13)) MPa for the exposure classes
213 XS3 and XD3 even at w/b = 0.55. However, for mix B10 the setting time was inconveniently short, at
214 around half an hour. Mixes B6(6%-0.45) and B8(4%-1) seem to meet the strength requirements of 43.11
215 (=37+1.48(4.13)) MPa for the exposure classes XS1, XD1 and XD2. Although it was evident that the
216 strength requirement and w/b ratio of mixes B1, B2, B3 and B5 will not comply with BS EN 206:2013
217 norms, the intention of including these mixes was to assess their performance against chloride ingress
218 and compare that data against a conforming PC reference.

219 Figure 5 shows the 91-day compressive strength results as a function of the SiO₂ content of the activator,
220 relative to the total slag content (calculated for each mix as Na₂O% × Ms). When the 91-day compressive
221 strength values of all the activated slag concrete mixes studied are plotted as a function of (Na₂O% ×
222 Ms), a two-term exponential relationship can be fitted, as shown in Fig. 5. In general, there is an increase
223 in the 91-days compressive strength values with increase in the SiO₂ content, up to a value of ~ 9% of
224 the total slag content. This parameter is significant because it has been shown that the later-age
225 compressive strengths of activated slag concretes are proportional to the SiO₂ content of the activator
226 [23], and a higher silicate content in the activator has been reported to lead to a higher degree of reaction
227 [24]. In agreement with this observation, the results here support the use of the maximum SiO₂ content
228 for optimising strength.

229 3.3 Chloride diffusivity through AASC

230 Figure 6 presents chloride diffusion coefficients, D_{nssd} , for mixes from both stages. Stage A mixes, at
231 w/b = 0.47, show very low to low chloride diffusivity values as identified in the classification of RILEM
232 TC 230-PSC [24], from 1.88×10^{-12} m²/s [A7 (8%-1.5)] to 6.59×10^{-12} m²/s [A1 (4%-0.75)]. Stage B
233 mixes, with w/b values of 0.55-0.7, demonstrate low to very low chloride diffusivity values [25], from
234 5.09×10^{-12} m²/s (B4) to 1.18×10^{-12} m²/s (B2). All of the coefficients obtained, with the exception of
235 A1, were lower than 6×10^{-12} m²/s, which is the lowest limiting value specified for the equivalent
236 durability approach in PD CEN/TR 16563 [26] for chloride environments. The coefficients obtained in
237 this study are also similar to the non-steady state chloride migration coefficient values measured via NT
238 Build 492 and reported elsewhere [27-29]. Comparing the results of the two stages illustrates that
239 despite the high w/b ratio, stage B concretes offer lower diffusion coefficients. This could be due to
240 better workability and compaction in the case of stage B mixes. All the D_{nssd} values for AAS concretes

241 were lower than the result shown for PC concrete in Figure 6(a), despite the higher water to binder ratio
242 of the AASC mixes. This is possibly due to the influence of the activated aluminosilicates, chloride
243 binding, pore size and pore connectivity of the concrete.

244 The effects of w/b and binder content are not directly obvious from the results. It seems that the excess
245 water is not affecting the pore structure/connectivity of AASC as it does for PC concrete. Therefore, it
246 can only be identified that mix design parameters and also reactivity of the aluminosilicate precursor
247 [30] may have a larger influence on the diffusivity.

248 The contour plot in Figure 7(a) (stage A) indicates that for lower w/b an optimum can be achieved by
249 increasing the $\text{Na}_2\text{O}\%$ and bringing the modulus closer to 1.5. The information in Figure 7(b) for stage
250 B gives a lower range: (i) for Na_2O doses less than 5%, the lowest value is observed at a higher M_s ,
251 similar to the observations in Figure 7(a), and (ii) for higher Na_2O doses, this is reversed.

252 In summary, the D_{nsd} is comparatively low for all of the AASC mixes studied here. D_{nsd} is a measure
253 of the rate of transport as modified by the chemical reactions leading to chloride binding. In order to
254 distinguish these two effects, the binding capacity of the mixes in stage B was assessed to develop a
255 more complete picture of the factors controlling chloride transport in AASC.

256 3.4 Chloride binding in AASC

257 There is limited information available on chloride binding of AASC in the literature. The available CSH
258 and aluminate phases (C-(N)-A-S-H or two layered double hydroxides) in activated GGBS may
259 contribute to the physical and chemical binding reactions [30, 31]. Figure 8 shows the total and water-
260 soluble chloride concentrations measured for concrete mixes B8, B9 and B10, and the corresponding
261 pH values are also provided for comparison. It is evident from Figure 8 that the surface region, Zone 1,
262 is undergoing leaching-induced changes during Cl^- transport that result in a lowering of pH; there is
263 also a skin effect which causes a near-surface dip in the total Cl^- content. The depth of zone 1 is between
264 5-12 mm for the three mixes; the lowest depth is for the mix with 6% Na_2O and $M_s = 1$. In Zone 2, pH
265 reduction is not significant. It is known that pH reduction can release the Cl^- otherwise bound to
266 Friedel's salt [32] in PC based systems. It should be noted that the total Cl^- is composed of both bound
267 and free chloride, and free chloride is represented here by the water soluble fraction which therefore
268 will also contain a proportion of the adhered Cl^- physically bound to the aluminate phases. The ratio
269 between total and water-soluble Cl^- seems to follow the general trends established for PC systems [33].
270 The quantity of bound chlorides for all the mixes in stage B is shown in Table 5. This is computed by
271 determining the area under the total and free chloride curves from the concentration vs depth graph
272 (typical data shown in Fig. 8); the difference between the two areas gives the quantity of bound chloride.
273 The values presented in Table 5 show that quantity of bound chlorides increased as the paste content of
274 the concrete and/or the silica content of the activator was increased. As discussed, the main reaction
275 product in AASC is an Na-Al substituted calcium silicate hydrate (C-(N)-A-S-H) gel which can bind

276 chlorides, while hydrotalcite-group minerals are a smaller constituent of the phase assemblage but have
277 strong chloride binding capacity. Surface absorption is the main binding mechanism in these phases,
278 responsible for around 90% of the total chloride uptake, with around 10% contribution from ion
279 exchange [30, 31]. The binding capacity is comparable to the values reported for PC and high-volume
280 blast furnace slag concrete [34]. This is likely due to the alkalinity reduction affecting the stability of
281 the bound chlorides [34, 35] in zone 1.

282 In summary, the mass transport testing showed that AASC performed significantly better than
283 conventional PC based binders in terms of restricting Cl^- transport. These concretes can be classified
284 into two zones, based on the reduction of pH closer to the surface. While the overall binding capacity
285 is deemed slightly lower than comparable PC systems, further study is needed to exclude the effect of
286 pH reduction and to eliminate near-surface effects.

287 **4. Conclusion**

- 288 • AAS concretes can be designed for different workability and strength grades of concrete. The
289 key parameters at the disposal of the designer are $\text{Na}_2\text{O}\%$, Ms, and the paste content.
- 290 • For higher water to binder ratio, both sodium oxide ($\text{Na}_2\text{O}\%$) and silica modulus (Ms) influence
291 the workability, while for lower w/b only $\text{Na}_2\text{O}\%$ seems to have a notable effect.
- 292 • The compressive strength values were strongly proportional to the SiO_2 content in the activator.
293 This will be useful as guidance to produce AASC of required strength.
- 294 • Chloride diffusion coefficients of AAS concretes are low. Measurement of chloride binding
295 capacity was affected by the pH reduction due to leaching in the surface zone. The depth of the
296 affected zone was in the range of 5-12 mm, so further study is required to discern the binding
297 capacity of zones unaffected by this type of pH reduction.
- 298 • The diffusivity results demonstrate that the excess water is not affecting the pore
299 structure/connectivity in AASC as it does for PC concretes; and AASC can be designed based
300 on the w/b needed for a required mechanical performance.

301 As a closing remark the authors suggest adopting a performance-based approach to specifying such
302 concretes, since the conventional wisdom of w/b and mix design features may not translate well [26].
303 A performance-based approach is apt to give confidence to the suppliers, and also to convince clients
304 of the beneficial aspects of AASC.

305

306

307

308

309 Table 1: Oxide composition of the GGBS used, from X-ray fluorescence analysis

Precursor	Component (mass % as oxide)							
	SiO ₂	Al ₂ O ₃	CaO	Fe ₂ O ₃	MgO	TiO ₂	Other	LOI*
GGBS	35.7	11.2	43.9	0.3	6.5	0.512	1.578	0.31

310 * LOI is loss on ignition at 1000°C.

311 Table 2: Physical properties of the GGBS used

Fineness (particles $\geq 45\mu\text{m}$)	7.74%
Particle density	2.86
Water absorption	35.14%

312

313 Table 3: Physical properties of aggregates

Aggregates	Bulk dry specific gravity	Bulk saturated surface-dry specific gravity	Water absorption (%)
Sand (0-4 mm)	2.72	2.73	0.75
Fine crushed agg. (5-10 mm)	2.67	2.75	3.14
Coarse crushed agg. (10-16 mm)	2.60	2.67	2.60

314

315 Table 4 (a): The details of the different Stage A mixtures and their properties

Mix No.	Mix details (Na ₂ O%-Ms)	Wet density	Setting time (initial/final) (min)	Slump (mm)	3 days compressive strength (MPa)	28 days compressive strength (MPa)	Concrete grade
A1	4%-0.75	2245	30/39	55	22.3	44.7	C32/40
A2	4%-1	2217	11/14	55	21.8	46.7	C35/45
A3	4%-1.5	2229	15/22	55	1.7	49.5	C35/45
A4	4%-2	2186	18/24	55	1.4	33.3	C30/37
A5	6%-0.75	2222	28/38	65	31.7	47.3	C35/45
A6	6%-1	2219	12/22	65	37.3	53.6	C40/50
A7	6%-1.5	2221	14/22	65	20.3	60.8	C49/60
A8	6%-2	2236	32/42	75	8	59.6	C45/55
A9	8%-0.75	2208	16/26	70	32.3	51.9	C40/50
A10	8%-1	2230	46/58	105	32.7	53.6	C40/50
A11	8%-1.5	2233	37/56	145	34.1	59.3	C45/55
A12	8%-2	2241	-	180	11.7	55.4	C45/55
A13	PC	2257	-	50	35.4	58.9	C45/55

316 Note: all mixes have a water to binder ratio of 0.47, binder content of 400 kg/m³, sand content of 670±16 kg/m³ and
 317 aggregate content of 1190±30 kg/m³, as outlined elsewhere [9]. The setting time for the alkali activated slag pastes based on
 318 standard consistence test (0.2<w/b<0.27) was studied in satge A and the results are reported in the above table. Due to the
 319 rapid setting observed, a retarder described in section 2.2 at a dosage of 0.3% (of the mass of slag) was used to control the
 320 setting of the AASC mixes. This dosage was the minimum to guarantee that the alkali activated slag mixes meet the setting
 321 time requirement specified in BS EN 197-1 (2011) [36, 37].

322

323

Table 4 (b): The details of the different Stage B mixtures and their properties

Mix No.	Mix (Na ₂ O%-Ms)	Binder (kg/m ³)	w/b	Sand (kg/m ³)	Aggregate (kg/m ³)	Wet density	Final setting time (min)	Slump (mm)	2 days compressive strength (Mpa)	28 days compressive strength (MPa)	Concrete grade
B1	4%-0.45	300	0.60	772	1158	2426	120	40	15.3	27.1	C20/25
B2	4%-0.45	360	0.70	671	1007	2410	145	225	11.1	21.5	C16/20
B3	4%-0.45	400	0.60	669	1004	2390	165	215	15.3	26.4	C20/25
B4	4%-0.45	400	0.55	701	1051	2395	160	168	17.8	30	C25/30
B5	6%-0.45	400	0.60	669	1004	2389	130	215	21.2	35.8	C28/35
B6	6%-0.45	400	0.55	701	1051	2469	125	135	24.7	44	C32/40
B7	8%-0.45	400	0.55	701	1051	2464	90	225	38.4	53.6	C40/50
B8	4%-1	400	0.55	701	1051	2519	80	160	25.8	47.8	C35/45
B9	6%-1	400	0.55	701	1051	2447.5	60	203	33.9	62.7	C49/60
B10	8%-1	400	0.55	701	1051	2420	40	240	33.7	64.4	C49/69

324 Note: The setting time of the AASCs in sage B are as reported in the above table and are based on observations during
 325 casting of concrete.

326

327

328

329

Table 5: Total Cl⁻, free Cl⁻, and bound Cl⁻ values for stage B mixes

Mix No.	Mix details (Na ₂ O%-Ms)	Binder (kg/m ³)	w/b	Total Cl ⁻ (Quantity)	Free Cl ⁻ (Quantity)	Bound Cl ⁻ (Quantity)
B1	4%-0.45	300	0.60	7.08	2.93	4.15
B2	4%-0.45	360	0.70	7.14	2.59	4.55
B3	4%-0.45	400	0.60	10.32	4.02	6.30
B4	4%-0.45	400	0.55	13.53	3.54	9.99
B5	6%-0.45	400	0.6	12.71	4.54	8.17
B6	6%-0.45	400	0.55	10.69	4.01	6.68
B7	8%-0.45	400	0.55	7.72	3.14	4.58
B8	4%-1	400	0.55	11.37	4.62	6.75
B9	6%-1	400	0.55	11.36	3.69	7.67
B10	8%-1	400	0.55	9.32	3.53	5.79

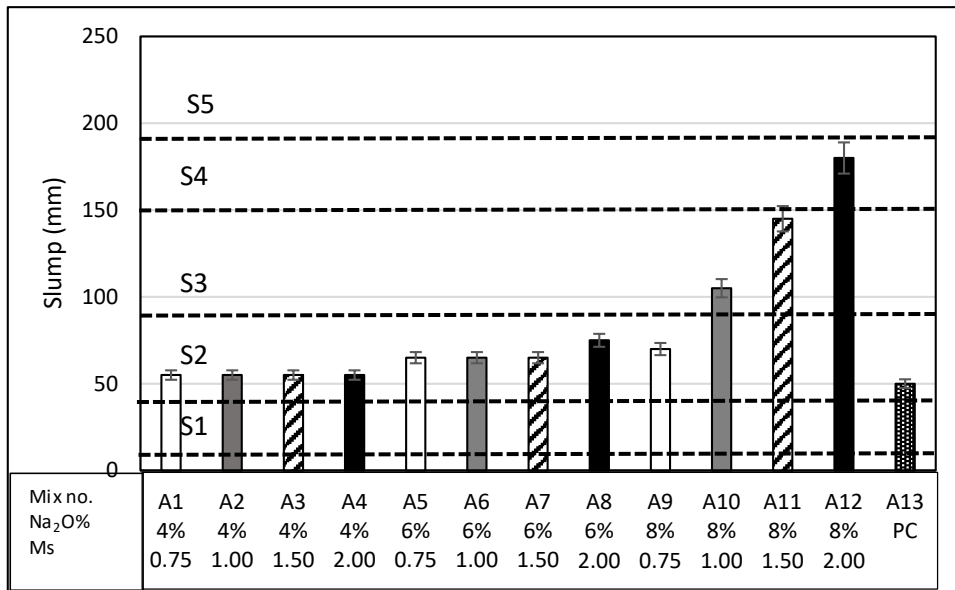
330 **Note:** Quantity of total Cl⁻ and free Cl⁻ was estimated by computing the area under the concentration vs depth
 331 curve. Maximum value for depth was 16mm for all mixes. Quantity of bound chlorides is therefore the difference
 332 between the total and free chlorides.

333

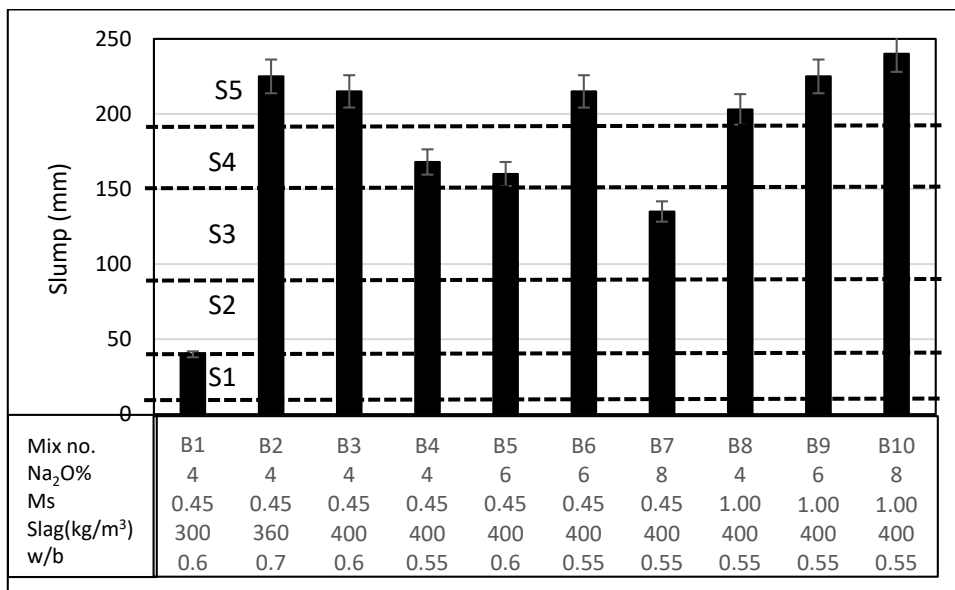
334

335

336

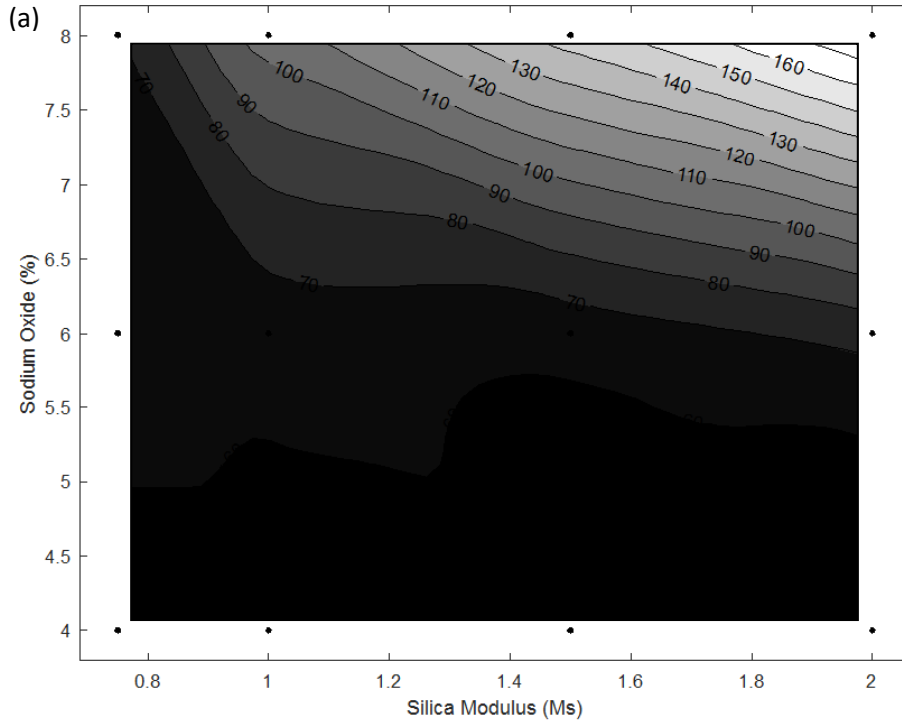


(a)

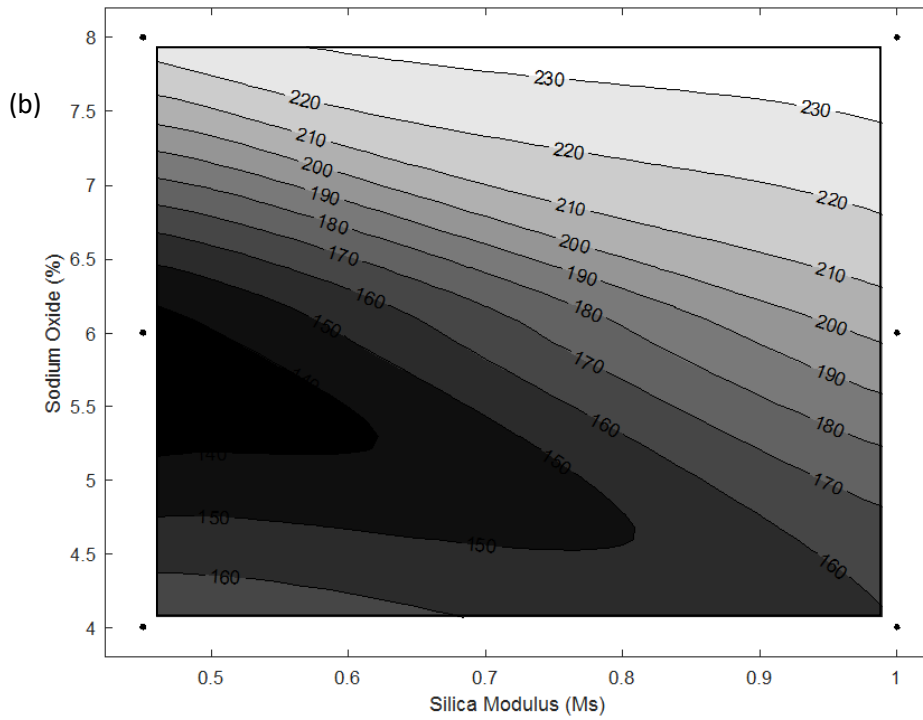


(b)

Figure 1. Slump results of AAS concretes: (a) Stage A, water to binder ratio = 0.47 and binder content = 400 kg/m³; (b) Stage B with various mix design parameters as marked

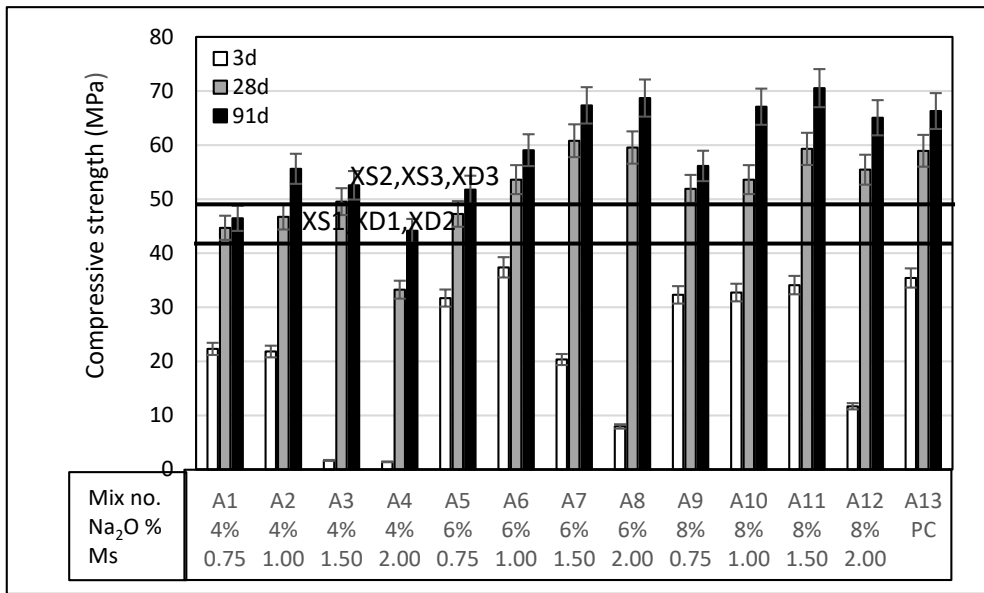


344

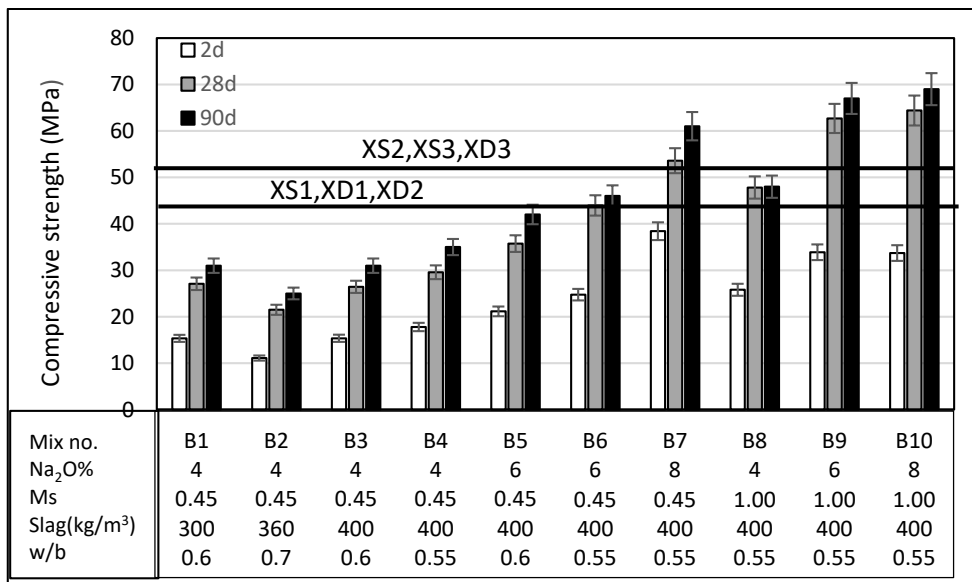


345

346 Figure 2. Contour graph for workability of different mixes (binder content=400 kg/m³): (a) Stage A,
 347 water to binder ratio = 0.47; (b) Stage B, water to binder ratio = 0.55



(a)

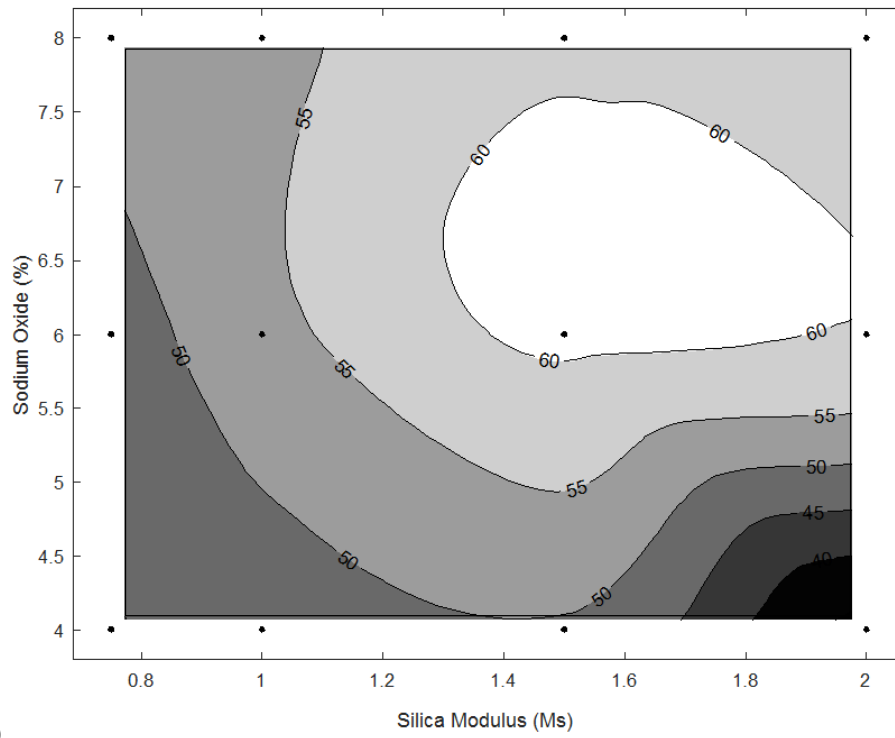


(b)

Figure 3. Strength results of AAS concretes at different curing ages: (a) Stage A, water to binder ratio = 0.47 and binder content = 400 kg/m³; (b) Stage B with various mix design parameters as marked. The error bar compare the difference between the mean with the amount of scatter within replicates.

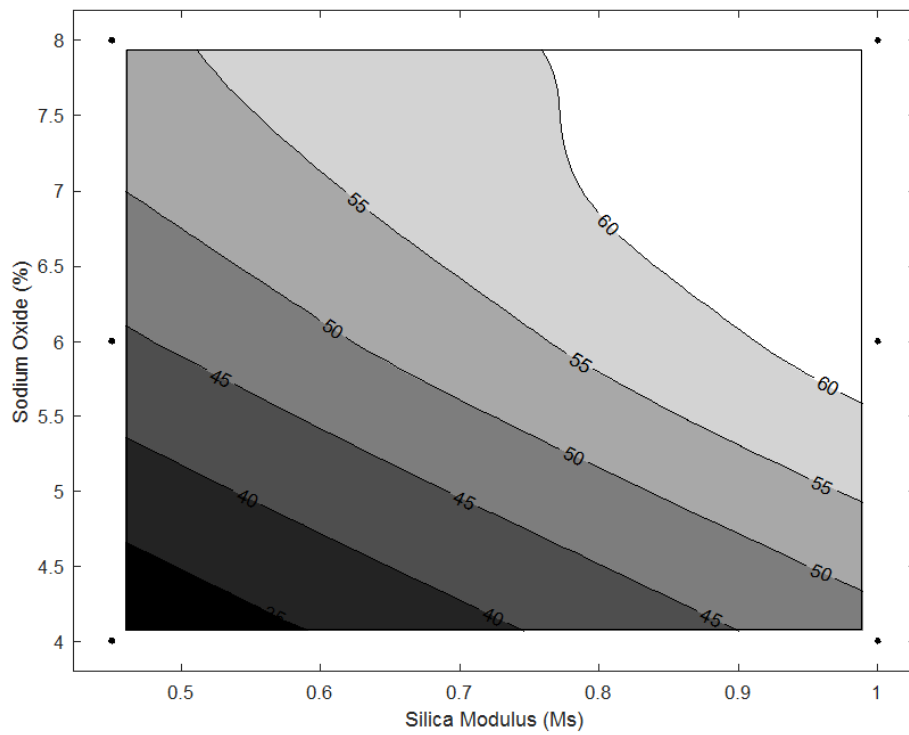
362

(a)



363

(b)



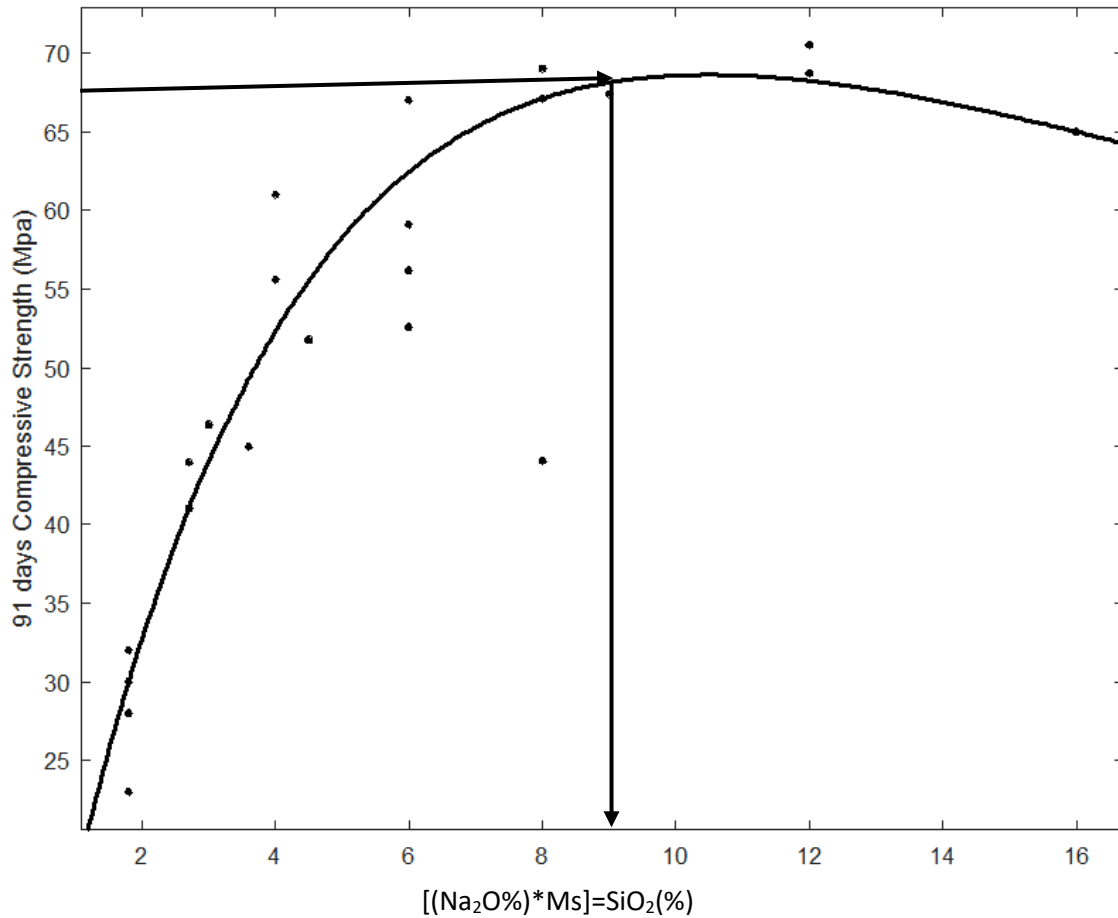
364

365

366

367

Figure 4. Contour graph for 28 days compressive strength of different mixes (binder content = 400 kg/m³): (a) Stage A, water to binder ratio = 0.47; (b) Stage B, water to binder ratio = 0.55.



368

369 Figure 5. Correlation of 91 days compressive strength and SiO₂ content in activator of AAS concrete

Fit found when optimization terminated:

General model Exp2:

$$f(x) = a \cdot \exp(b \cdot x) + c \cdot \exp(d \cdot x)$$

Coefficients (with 95% confidence bounds):

- a = 92.67 (16.16, 169.2)
- b = -0.02089 (-0.07184, 0.03005)
- c = -95.84 (-155.7, -35.99)
- d = -0.2671 (-0.539, 0.004749)

Goodness of fit:

- SSE: 312.5
- R-square: 0.9315
- Adjusted R-square: 0.9201
- RMSE: 4.166

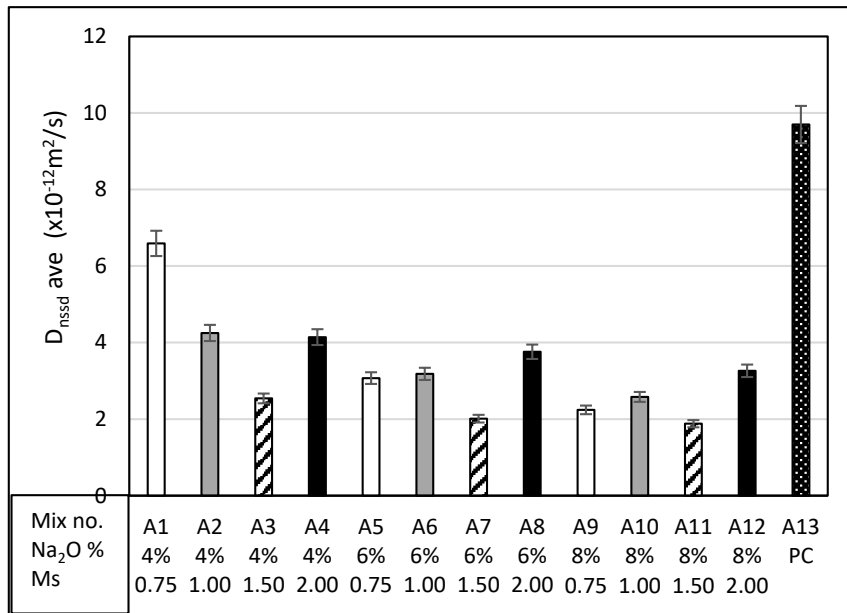
370

371

372

373

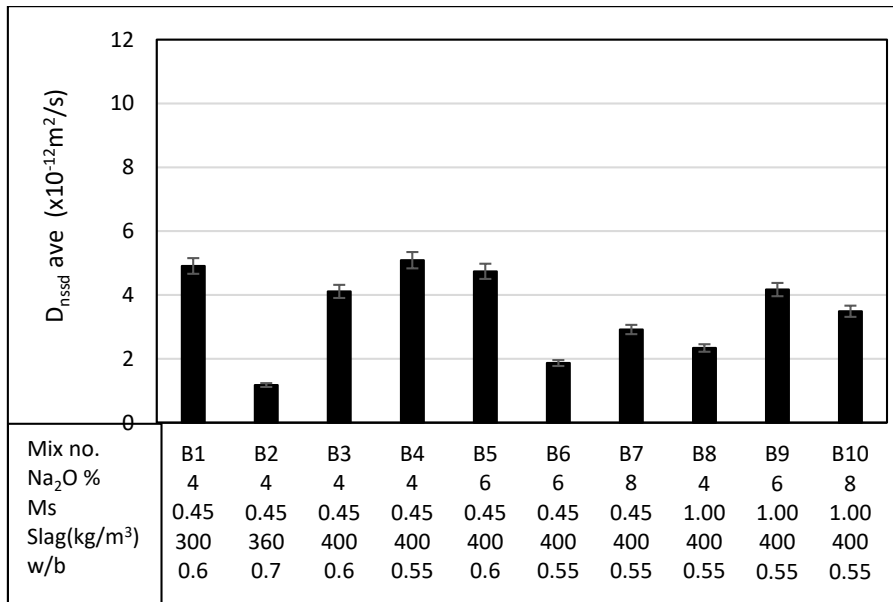
374



375

376

(a)



377

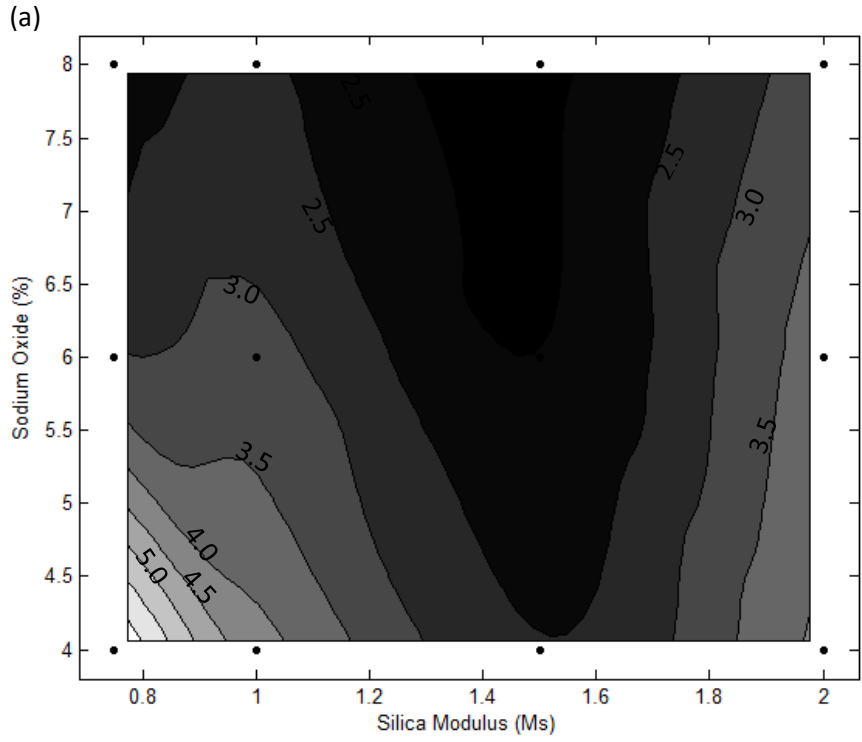
378

(b)

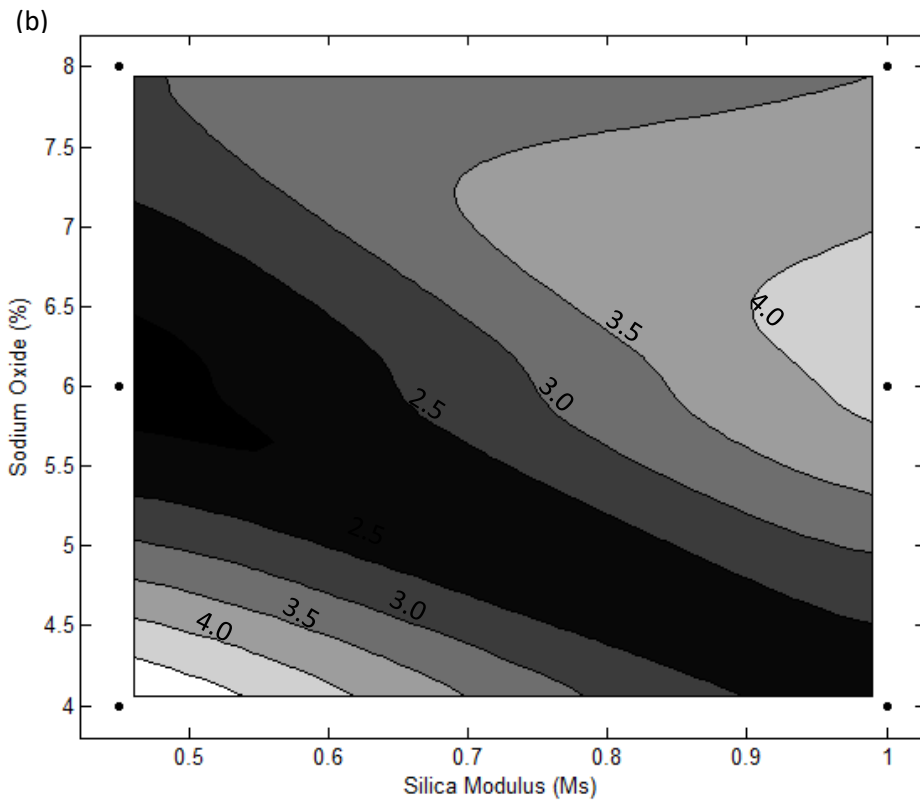
379

380

Figure 6 D_{nssd} values measured for AAS concrete mixes: (a) Stage A- water to binder ratio=0.47 and binder content = 400 kg/m³ (b) Stage B



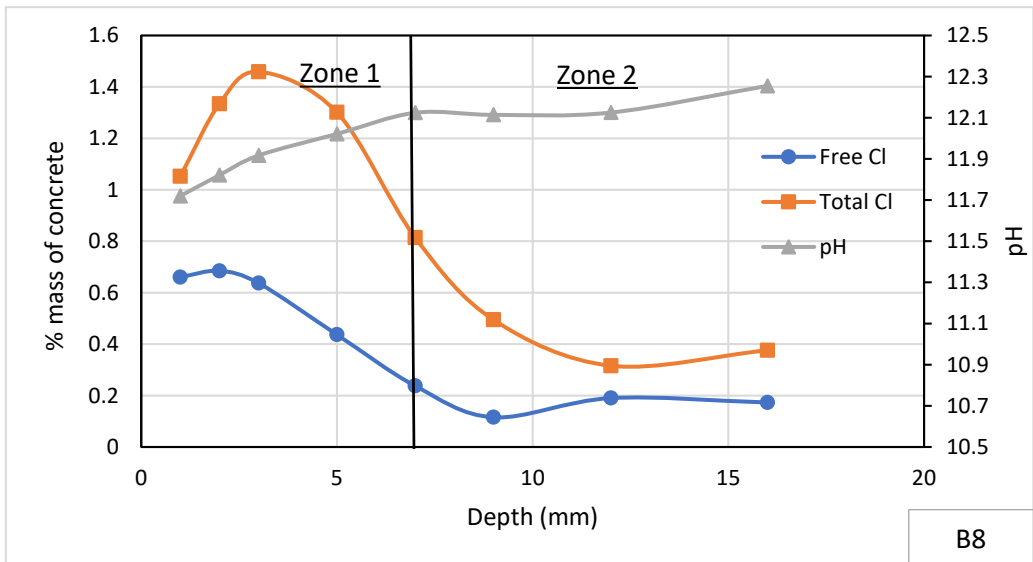
381



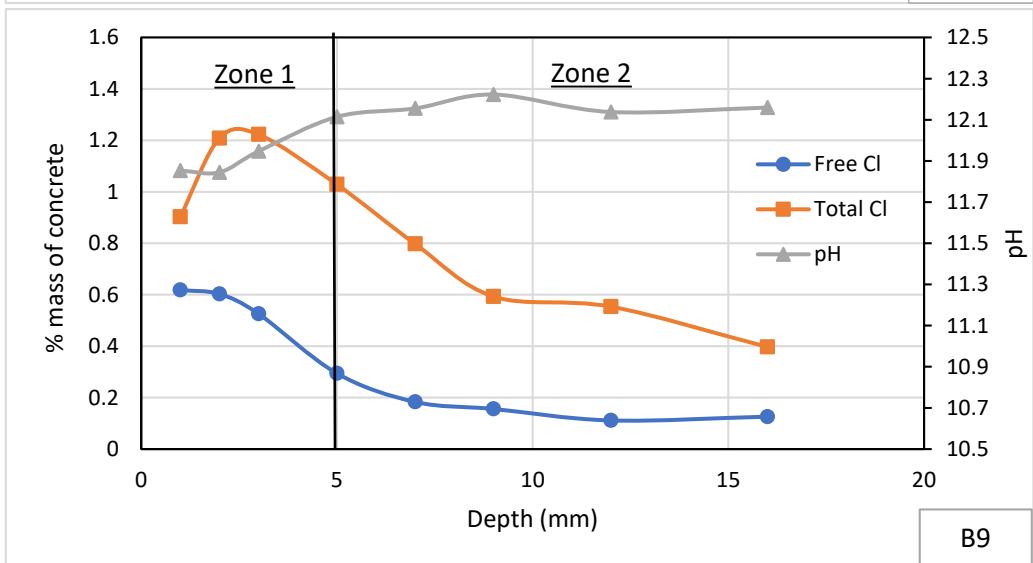
382

383 Figure 7 Contour graphs for D_{nssd} ($\times 10^{-12}$ m²/s) of different mixes (binder content = 400 kg/m³): (a)

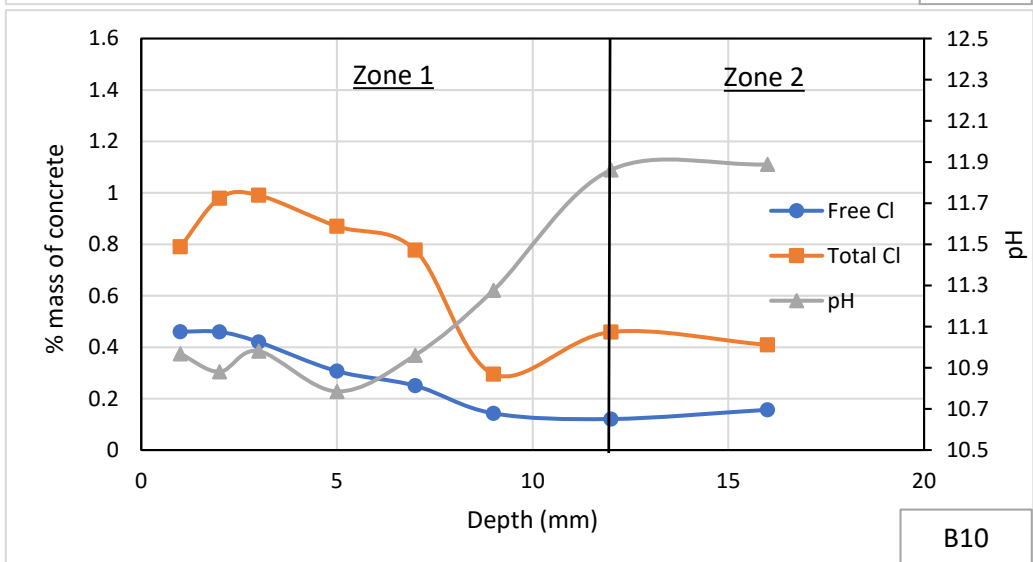
384 Stage A, water to binder ratio = 0.47; (b) Stage B, water to binder ratio = 0.55



385



386



387

388

389

390

Figure 8 Total and water-soluble Cl^- and pH of mixes B8, B9 and B10 of stage B

391 **Acknowledgements**

392 This work was supported by the United Kingdom Engineering and Physical Sciences Research Council
393 (EPSRC) under grant EP/M003272/1, awarded jointly with NSFC (China). The authors gratefully
394 acknowledge Dr. Y. Bai and Professor C. Yang for their technical guidance in data generated in stage
395 A of this work.

396 **References**

- 397 [1] Whiting, J., (1895), “Manufacture of Cement”, U.S. Patent 544,706
- 398 [2] Provis, J.L., van Deventer, J.S.J. eds., (2014), Alkali Activated Materials, State-of-the-Art Report,
399 RILEM TC 224-AAM. RILEM/Springer: Dordrecht.
- 400 [3] Wang, S.D., Scrivener, K.L., Pratt, P.L., (1994), “Factors affecting the strength of alkali-activated
401 slag”, Cement and Concrete Research, 24(6), 1033-1043
- 402 [4] Shi, C., Krivenko, D., Roy, P., (2006), Alkali Activated Cements and Concretes, Taylor &
403 Francis:London.
- 404 [5] Krizan, D., Zivanovic, B., (2002), “Effects of dosage and modulus of water glass on early hydration
405 of alkali-slag cements”, Cement and Concrete Research, 32 (8), 1181-1188
- 406 [6] Fernández-Jiménez, A., Puertas, F., (2003), “Effect of activator mix on the hydration and strength
407 behavior of alkali-activated slag cements”, Advances in Cement Research, 15(3), 129-136
- 408 [7] Bernal, S.A., Mejía de Gutiérrez, R., Pedraza, A.L., Provis, J.L., Rodríguez, E.D., Delvasto, S.,
409 (2011), “Effect of binder on the performance of alkali-activated slag concretes”, Cement and Concrete
410 Research, 41(1), 1-8
- 411 [8] Park, J.W., Ann, K.Y., Cho, C.G.(2015), “Resistance of alkali-activated slag concrete to chloride-
412 induced corrosion”, Advances in Materials Science and Engineering, Article ID 273101, 7 pages
- 413 [9] Ma, Q., Nanukuttan, S.V., Basheer, P.A.M., Bai, Y., Yang, C. (2016) “Chloride transport and the
414 resulting corrosion of steel bars in alkali activated slag concretes”, Materials and Structures, 49(9), 363-
415 3677
- 416 [10] BS EN 206 (2013) Concrete —Part 1: Specification, performance, production and conformity, BSI,
417 London
- 418 [11] BS 1881-125 (2013) Testing Concrete-Part 125: Methods for mixing and sampling fresh concrete
419 in the laboratory, BSI, London
- 420 [12] BS EN 12350-2 (2009) Testing fresh concrete - Part 2: Slump test, BSI, London
- 421 [13] BS EN 12390-3 (2009) Testing hardened concrete - Part 3: Compressive strength of test specimens,
422 BSI, London
- 423 [14] NT BUILD 443 (1995) Concrete, hardened: accelerated chloride penetration, NORDTEST, Espoo.
- 424 [15] RILEM TC 178-TMC: “Testing and modelling chloride penetration in concrete. Analysis of total
425 chloride content in concrete, recommendation”, Materials and Structures (2002), 35, 583-585
- 426 [16] RILEM TC 178-TMC: “Testing and modelling chloride penetration in concrete. Analysis of water
427 soluble chloride content in concrete, recommendation”, Materials and Structures (2002), 35, 586-588
- 428 [17] Collins, F.G., Sanjayan, J.G., (1999) “Workability and mechanical properties of alkali activated
429 slag concrete”, Cement and Concrete Research, 29(3), 455-458

- 430 [18] BS 8500-1 (2015) Concrete—complementary British Standard to BS EN 206-1—part 1: method
431 of specifying and guidance for the specifier, BSI, London
- 432 [19] Allahverdi, A., Shaverdi, B., Najafi Kani, E., (2010) “Influence of sodium oxide on properties of
433 fresh and hardened paste of alkali-activated blast-furnace slag”, *International Journal of Civil*
434 *Engineering*, 8(4), 304-314
- 435 [20] Yang, T.R., Chang, T.P., Chen, B.T., Shih, J.Y., Lin, W.L. (2012) “Effect of alkaline solutions on
436 engineering properties of alkali-activated GGBFS paste”, *Journal of Marine Science and Technology*,
437 20(3), 311-318
- 438 [21] Krizan, D., Zivanovic, B., (2002), “Effect of dosage and modulus of water glass on early hydration
439 of alkali slag cement”, *Cement and Concrete Research*, 32(8), 1181-1188
- 440 [22] Winnefeld, F., Ben Haha, M., Le Saout, G., Costoya, M., Ko, S.-C., Lothenbach, B. (2015)
441 “Influence of slag composition on the hydration of alkali-activated slags”, *Journal of Sustainable*
442 *Cement-Based Materials*, 4(2), 85-100.
- 443 [23] Ravikumar, D., Neithalath, N., (2012), “Effects of activator characteristics on the reaction product
444 formation in slag binders activated using alkali silicate powder and NaOH”, *Cement and Concrete*
445 *Composites* 34(7), 809-818
- 446 [24] Lloyd, R.R., Provis, J.L., van Deventer, J.S.J., (2010), “Pore solution composition and alkali
447 diffusion in inorganic polymer cement”, *Cement and Concrete Research*, 40(9), 1386-1392
- 448 [25] Beushausen, H., Fernandez Luco, L. eds, (2016) *Performance-Based Specifications and Control of*
449 *Concrete Durability, State-of-the-Art Report, RILEM TC 230-PSC, RILEM/Springer: Dordrecht.*
- 450 [26] PD CEN/TR 16563 (2013) *Principles of the equivalent durability procedure*, CEN, Brussels.
- 451 [27] van Deventer, J.S.J., San Nicolas, R., Ismail, I., Bernal, S. A., Brice, D. G., Provis, J. L., (2014)
452 “Microstructure and durability of alkali-activated materials as key parameters for standardization”,
453 *Journal of Sustainable Cement-Based Materials*, 4(2), 116-128
- 454 [28] Ravikumar, D., Neithalath, N., (2013), “Electrically induced chloride ion transport in alkali
455 activated slag concretes and the influence of microstructure”, *Cement and Concrete Research* 47, 31-
456 42
- 457 [29] Ismail, I., Bernal, S. A., Provis, J. L., San Nicolas, R., Brice, D. G., Kilcullen, A. R., Hamdan, S.,
458 van Deventer, J. S.J., (2013) “Influence of fly ash on the water and chloride permeability of alkali-
459 activated slag mortars and concretes”, *Construction and Building Materials*, 48, 1187–1201
- 460 [30] Ke, X., Bernal, S. A., Provis, J. L., (2017) “Uptake of chloride and carbonate by Mg-Al and Ca-Al
461 layered double hydroxides in simulated pore solutions of alkali-activated slag cement”, *Cement and*
462 *Concrete Research* 100, 1–13
- 463 [31] Ke, X., Bernal, S. A., Hussein, O. H., Provis, J. L., (2017) “Chloride binding and mobility in
464 sodium carbonate-activated slag pastes and mortars”, *Materials and Structures*, 50: #252
- 465 [32] Backus, J., McPolin, D., Basheer, M., Long, A., Holmes, N. (2013), “Exposure of mortars to cyclic
466 chloride ingress and carbonation”, *Advances in Cement Research*, 25(1), 3-11
- 467 [33] Castellote, M., Andrade, C., Alonso, C., (1999) “Chloride-binding isotherms in concrete submitted
468 to non-steady-state migration experiments”, *Cement and Concrete Research*, 29, 1799-1806
- 469 [34] Tang, L., Nilsson, L., (1993) “Chloride binding capacity and binding isotherms of OPC pastes and
470 mortars”, *Cement and Concrete Research*, 23(2), 247– 253

- 471 [35] Luo, R., Cai, Y., Wang, C., Huang, X., (2003) “Study of chloride binding and diffusion in GGBS
472 concrete”, *Cement and Concrete Research*, 33(1), 1 –7
- 473 [36] BS EN 197-1 (2011) Cement. Composition, specifications and conformity criteria for common
474 cements (incorporating corrigenda November 2011 and October 2015), BSI, London
- 475 [37] Ma, Q. (2013), Chloride transport and chloride induced corrosion of steel reinforcement in sodium
476 silicate solution activated slag concrete, PhD Thesis, Queens University of Belfast, Northern Ireland,
477 UK.